Atomistic origins of the phase transition mechanism in $Ge_2Sb_2Te_5$

Juarez L. F. Da Silva,[1,2,a)] Aron Walsh,[3] Su-Huai Wei,[1] and Hosun Lee[4]
[1]*National Renewable Energy Laboratory, 1617 Cole Blvd., Golden, Colorado 80401, USA*
[2]*Instituto de Física de São Carlos, Universidade de São Paulo, Caixa Postal 369, São Carlos, 13560-970 São Paulo, Brazil*
[3]*Department of Chemistry, Materials Chemistry, University College London, London WC1H 0AJ, United Kingdom*
[4]*Department of Applied Physics, Kyung Hee University, Suwon 446-701, South Korea*

(Received 8 September 2009; accepted 21 October 2009; published online 4 December 2009)

The fast and reversible phase transition mechanism between crystalline and amorphous phases of $Ge_2Sb_2Te_5$ has been in debate for several years. Through employing first-principles density functional theory calculations, we identify a direct structural link between the metastable crystalline and amorphous phases. The phase transition is driven by the displacement of Ge atoms along the rocksalt [111] direction from stable octahedron to high energy unstable tetrahedron sites close to the intrinsic vacancy regions, which generates a high energy intermediate phase between metastable and amorphous phases. Due to the instability of Ge at the tetrahedron sites, the Ge atoms naturally shift away from those sites, giving rise to the formation of local-ordered fourfold motifs and the long-range structural disorder. Intrinsic vacancies, which originate from Sb_2Te_3, lower the energy barrier for Ge displacements, and hence, their distribution plays an important role in the phase transition. The high energy intermediate configuration can be obtained experimentally by applying an intense laser beam, which overcomes the thermodynamic barrier from the octahedron to tetrahedron sites. The high figure of merit of $Ge_2Sb_2Te_5$ is achieved from the optimal combination of intrinsic vacancies provided by Sb_2Te_3 and the instability of the tetrahedron sites provided by GeTe. © *2009 American Institute of Physics*. [doi:10.1063/1.3264883]

I. INTRODUCTION

Volatile random access memory (RAM) devices are widely used in modern electronics. While they are faster than nonvolatile memory devices based on magnetic storage such as hard disks, information in the RAM is only preserved while the device is powered. Thus, there is a desire to develop stable nonvolatile RAM, which can simultaneously achieve fast and large storage capacities.[1] The resistance-change memory concept has attracted great interest for this purpose, which relies on the change in current flow through low- and high-resistivity regions of a material to store information (bits).[2] In this context, ternary $(GeTe)_m(Sb_2Te_3)_n$ materials, in particular, the $Ge_2Sb_2Te_5$ (GST) composition, have been considered as the most natural candidates for nonvolatile memory applications through exploiting the fast and reversible phase change between a crystalline phase (low resistivity) and an amorphous phase (high resistivity).[2–6] GST has demonstrated high figures of merit for multimedia storage applications resulting in its use in rewritable compact disks (CD-RW), digital versatile disks (DVD), and blu-ray disks (BD); however, an atomic-level understanding of the mechanism that drives the phase transition between both crystalline and amorphous phases is still under intense debate. This compromises the effort to improve upon current GST performance by using different compositions of GeTe and Sb_2Te_3,[7] nanoparticles,[8] and the design of alternative phase change materials.[9]

The process in which information is written and erased in rewritable optical storage devices can be described as follows.[3,5,10–14] A short and focused pulse of a high-intensity laser beam heats an encapsulated crystalline thin GST film (about 10 nm thickness) above its melting temperature, and a liquidlike state is formed in a tiny region of the film. Rapid cooling (10^9 K s^{-1}) quenches the liquidlike state into a disordered amorphous phase. The amorphous and crystalline phases have different optical contrasts, which have been widely discussed,[15–22] and hence, both regions can be detected by a low-intensity laser beam. The erasing process is performed by inducing a phase transition of the amorphous phase located in the tiny region into a crystalline phase, which is achieved by using an intermediate power laser beam. The laser heats the amorphous regions in the thin film above the crystallization temperature, in which the atoms become mobile and revert to the crystalline phase. Thus, three states can be distinguished in the writing and erasing processes, namely, crystalline, liquidlike, and amorphous (a-GST) phases.

The GST compound, as well as other compositions, crystallizes in two well known phases, namely, the stable hexagonal[23–31] (s-GST) and metastable rocksalt (RS) (m-GST) phases. Experimental studies indicate that only the m-GST phase takes part in optical storage applications;[3,5,10–14] however, both structures have very similar structure features as discussed by Da Silva *et al.*[32] employing first-principles calculations. The intrinsic vacancies, which originate from Sb_2Te_3, are present in both phases; however, the intrinsic vacancies occupy specific lattice sites only in the RS m-GST structure, while it only separate the

a)Electronic mail: dasilva_juarez@yahoo.com.

building GST blocks in the s-GST phase. A simple geometric analysis of the crystalline GST structures indicates that the distribution of the intrinsic vacancies might play an important role in the phase transition mechanism, which might explain why only the m-GST phase takes place in optical applications. In both phases, the Ge and Sb atoms are distributed in such a way that maximizes the number of Te atoms surrounded by three Ge and three Sb atoms (3Ge–Te–3Sb rule), which helps decrease the crystal energy.[32] In this work, we will restrict ourselves to the m-GST phase due to the key role that it plays in optical storage applications.[3,5,10–14]

Experimental techniques such as high-resolution transmission electron microscopy (HRTEM), x-ray diffraction study (XRD), extended x-ray absorption fine-structure spectroscopy (EXAFS), and theoretical studies for the m-GST[27–29,31–49] phase have reported that the Te atoms occupy the anion sites and Ge, Sb, and the intrinsic vacancies (20% in GST) occupy the cation sites in the RS structure. Despite the seeming simplicity, the structural details of the m-GST structure are still under intense debate. First-principles calculations have found that the intrinsic vacancies form ordered (111) planes,[32,40] which confirm previous experimental studies based on HRTEM.[38] However, there is also strong evidence for a random distribution of the intrinsic vacancies at high energy configurations,[34] which might depend on the cooling rate from amorphous to crystalline.[50] XRD studies suggest that cations occupy ideal high-symmetry RS lattice sites;[34] however, EXAFS studies[37] suggested that the Ge and Sb atoms are shifted from their ideal RS sites in a strongly correlated manner with respect to the neighboring Te atoms; i.e., m-GST may adopt a distorted RS structure such as GeTe.[51,52] The latter interpretation is supported by recently first-principles calculations reported by Da Silva *et al.*,[32] which is also consistent with previous studies for bulk GeTe in the distorted RS structure.[51,52]

Based on experimental and theoretical studies, it has been suggested that a-GST is characterized by the presence of fourfold coordinated Ge atoms,[37,42,46,48,50,53–60] in which the sum of the occurrences of $GeTe_4$, $Ge(SbTe_3)$, and $Ge(GeTe_3)$ is about 66%,[59] which is similar to the local environments observed in amorphous GeTe for $GeTe_4$ and $Ge(GeTe_3)$.[61] Ge–Ge and Ge–Sb bonds are found in those motifs, which is assumed to be due to disorder effects, since they are not present in the crystalline phases. Furthermore, a-GST shows volume expansion of 6%–7% compared with the m-GST phase,[10,36,62] and it has a higher energy (28–40 meV/at.) with respect to m-GST.[63] Based on EXAFS studies and Ge coordination change, Kolobov *et al.*[54] suggested that the m-GST to a-GST transition is related to an umbrella flip of Ge atoms from octahedral to tetrahedral sites without the rupture of strong covalent bonds. This suggestion has proved highly debatable as it cannot explain the existence of several features in the phase transition mechanism, e.g., existence of a high energy phase, the existence of Ge–Ge bonds.

Recently, Hegedüs and Elliott,[50] using first-principles molecular dynamics (MD) simulations at high temperature found that a RS-like structure can be formed from a liquid-like phase with slow cooling rates, which is expected, taking into account that m-GST has a lower energy than a-GST. However, due to the complex nature of the structures in both phases, a direct link between them was not clear. Moreover, it is also not clear why a slow cooling MD simulation yields the m-GST phase and not the s-GST, which has slightly lower energy than the m-GST. It is important to mention that both phases are semiconductors with optical band gaps from 0.50 (crystalline) to 0.70 eV (amorphous).[64]

Although previous studies have provided a very important advance in the understanding of the phase change mechanism in GST, knowledge of the underlying physical origin at the atomic scale is still starkly lacking. Is there a dominant structure link between both phases through an intermediate phase? What are the respective roles of GeTe and Sb_2Te_3 in the high figures of merit of GST? Why is there no direct phase transition from the ground-state crystalline GST phase (s-GST) to the amorphous phase? We address each of these questions and provide a clear understanding of the phase transition mechanism through the combination of static (zero temperature) and MD (high temperature) first-principles density functional theory (DFT) calculations for the GST compounds in the m-GST and a-GST phases. To provide further insight to the unusual GST behavior, calculations were also performed for the two binary components GeTe and Sb_2Te_3.

II. THEORETICAL APPROACH

A. Computational details

Our static total energy calculations and *ab initio* MD simulations are based on DFT[65,66] within the generalized gradient approximation (GGA) formulated by Perdew, Burke, and Erzenhof (PBE).[67] The Kohn–Sham equations were solved by the all-electron projected augmented wave method[68,69] as implemented in the Vienna *ab initio* simulation package (VASP).[70,71] Cut-off energies of 173, 288, and 576 eV were used for the MD, total energy, and stress tensor calculations, respectively, while for the Brillouin zone integration a $(3\times3\times1)$ **k**-point grid was used for GST in the RS-type structure using a hexagonal $(2\times2\times5)$ unit cell (a_0=8.53 Å and c_0=55.07 Å), which is discussed below. Similar quality **k**-points, i.e., the same density, were employed for all other calculations. All structures for both phases were modeled using unit cells up to 120 atoms.

B. Crystalline structures

As mentioned in the Introduction, m-GST crystallizes in a RS structure in which the Te atoms occupy the anion sites and the Ge, Sb, and intrinsic vacancies occupy the cation sites. Thus, a single f.u. of GST requires five cation and five anion sites. Analysis of the composition and the available number of lattice sites in the RS structure leads to the conclusion that the smallest commensurate cubic cell has 1000 sites (500 cations and 500 anions), which implies a high computational cost even for simple studies. Previous DFT studies have used smaller cubic unit cells;[39] however, those studies were performed for compositions such as $Ge_2Sb_2Te_{4.92}$, which cannot provide the correct description of GST as they do not preserve overall stoichiometry. Thus,

in order to reduce computational cost and achieve a correct physical description of GST, we employ supercells with hexagonal lattice vectors. For example, a primitive RS lattice can be written using a minimum commensurate hexagonal cell with six lattice sites. Hence, based on this notation, a $(1\times1\times5)$ hexagonal supercell has 30 sites, thus can accommodate 3 f.u. of m-GST. However, a $(1\times1\times5)$ cell implies that each layer has only a single species, but, experimental results have suggested that both Ge and Sb species might form intermixed layers,[29,31] while the intrinsic vacancies might be random distributed.[34] Thus, the selected unit cell should have enough sites to provide room for Ge and Sb intermixing among the layers and a possibility to test between ordered and slightly disordered distributions for the intrinsic vacancies. We find that the $(2\times2\times5)$ unit cell, which contains 120 sites, satisfy those basic physical requirements. The total energies and equilibrium volumes for all structures in both crystalline and amorphous phases were obtained by full relaxation of the volume, shape, and atomic positions (<0.01 eV/Å) of the unit cell to minimize the quantum mechanical stresses and forces.

C. Amorphous structures

For the simulation of a-GST, we employ two sets of unit cells, namely, a cubic cell within 8 f.u. and a hexagonal $(2\times2\times5)$ unit cell. To have a correct composition, the cubic cell was built up by adding interstitial atoms to the 64 atom $GeSb_2Te_4$ structure, while the hexagonal unit cell construction has been described above. Initially, we performed 50 ps at 3000 K to remove structure memory effects; i.e., no history present in the initial cubic and hexagonal cells was kept. Thus, the results obtained from both cells can be compared at the end as a cross-check to verify the convergence of the results. Once the history was removed, we performed a series of 20 ps runs from 3000 to 500 K, e.g., 20 ps from 3000 to 2000 K and 20 ps at 2000 K. Once the temperature of 500 K was reached, a 50 ps of equilibration was performed at 500 K. A time step of 4.0 fs was used, which was chosen to approach one-tenth of the highest vibrational frequency (Γ-point phonon) of the solid phases.[53] In order to improve the statistics of our simulations, which is required due to the finite time and cell scale, we selected several structures for both cells from the final equilibration run. These selected structures were then cooled for 20 ps from 500 to 100 K, and were then finally quenched to zero temperature.

D. Potential energy of GeTe along of the [111] direction

In order to explain our findings (see below), we calculated the potential energy of GeTe for Ge displacements along the [111] direction. For these calculations we employed a rhombohedral (primitive fcc) lattice, in which the angles between the primitive lattice vectors and volume are optimized using the stress tensor for fixed atomic positions of the Ge and Te atoms.

III. RESULTS

A. Metastable GST crystalline phase

As mentioned in the Introduction, the crystalline m-GST phase is a key component in optical storage applications.[3,5,10–14] Thus, knowledge of the atomic structure of m-GST is a basic requirement to obtain an atom-level understanding of the storage-erase process. We have previously identified the lowest energy m-GST structure, within a hexagonal $(2\times2\times5)$ unit cell, through examination of a large number of possible configurations;[32] the resulting structure is shown in Fig. 1(a). These results are discussed in detail in Ref. 32, and only the pertinent results relevant to this work will be discussed below.

In m-GST, intrinsic vacancies preferentially form ordered (111) planes, which is consistent with HRTEM results[38] and similar to the distribution of intrinsic vacancies found in its parent Sb_2Te_3 as well as the low energy s-GST phase. One distinction is that in s-GST, the intrinsic vacancies do not occupy lattice sites, but form vacancy planes perpendicular to the hexagonal [0001] direction and separate the building GST blocks.[23–31] Thus, the intrinsic vacancies are not randomly distributed in the lowest energy configurations. Calculations for a random distribution of the intrinsic vacancies in m-GST yield configurations with high energies (180–720 meV/f.u.), which will be more easily obtained from MD simulations compared to the ordered lowest energy configuration. This leads to the conclusion that the atomic structure of m-GST at room temperatures may not be unique, and hence, it might play an important role in facilitating the phase transition mechanism.

In the lowest energy configurations, the mGeTe and $n$$Sb_2Te_3$ units combine to form $(GeTe)_m(Sb_2Te_3)_n$ superlattices stacked along the hexagonal [0001] (RS [111]) direction, in which the mGeTe units are inserted into a single Sb_2Te_3 block, while the remaining $(n-1)Sb_2Te_3$ units form $(n-1)Sb_2Te_3$ blocks separated by ordered intrinsic vacancy layers like in Sb_2Te_3. The crystal energy is further lowered by maximizing the number of Te atoms surrounded by three Ge and three Sb atoms (3Ge–Te–3Sb rule) located in the opposite side of the octahedron structures. The Te atoms have a sequence along the [111] direction of ABCABC, which is typical of RS structures. Using the equilibrium lattice constants ($a_0=8.53$ Å and $c_0=55.07$ Å) for the hexagonal $(2\times2\times5)$ unit cell, and its relation to the RS lattice, we obtained a lattice constant of 6.20 Å for the RS structure, which is consistent with experimental results, namely, $a_0^{RS}=6.01-6.03$ Å.[33,34] Thus, we found deviations of about 2.7%, which is typical of DFT-PBE calculations for semiconductor and metal systems.[72,73]

The 3Ge–Te–3Sb rule leads to the intermixing of Ge and Sb atoms in the same (111) planes and the formation of two distinct bond lengths for Ge–Te (2.87 and 3.24 Å, $\Delta_b=0.37$ Å) and Sb–Te (2.96 and 3.30 Å, $\Delta_b=0.34$ Å), which are important finger prints to prove that our structure model for m-GST provides a correct description of the experimental findings. For example, Kolobov *et al.*[37] employing EXAFS identified two bond lengths in m-GST, i.e., 2.83 ± 0.01 and 3.2 ± 0.3 Å ($\Delta_b=0.37$ Å) for Ge–Te, and 2.91 ± 0.01 and

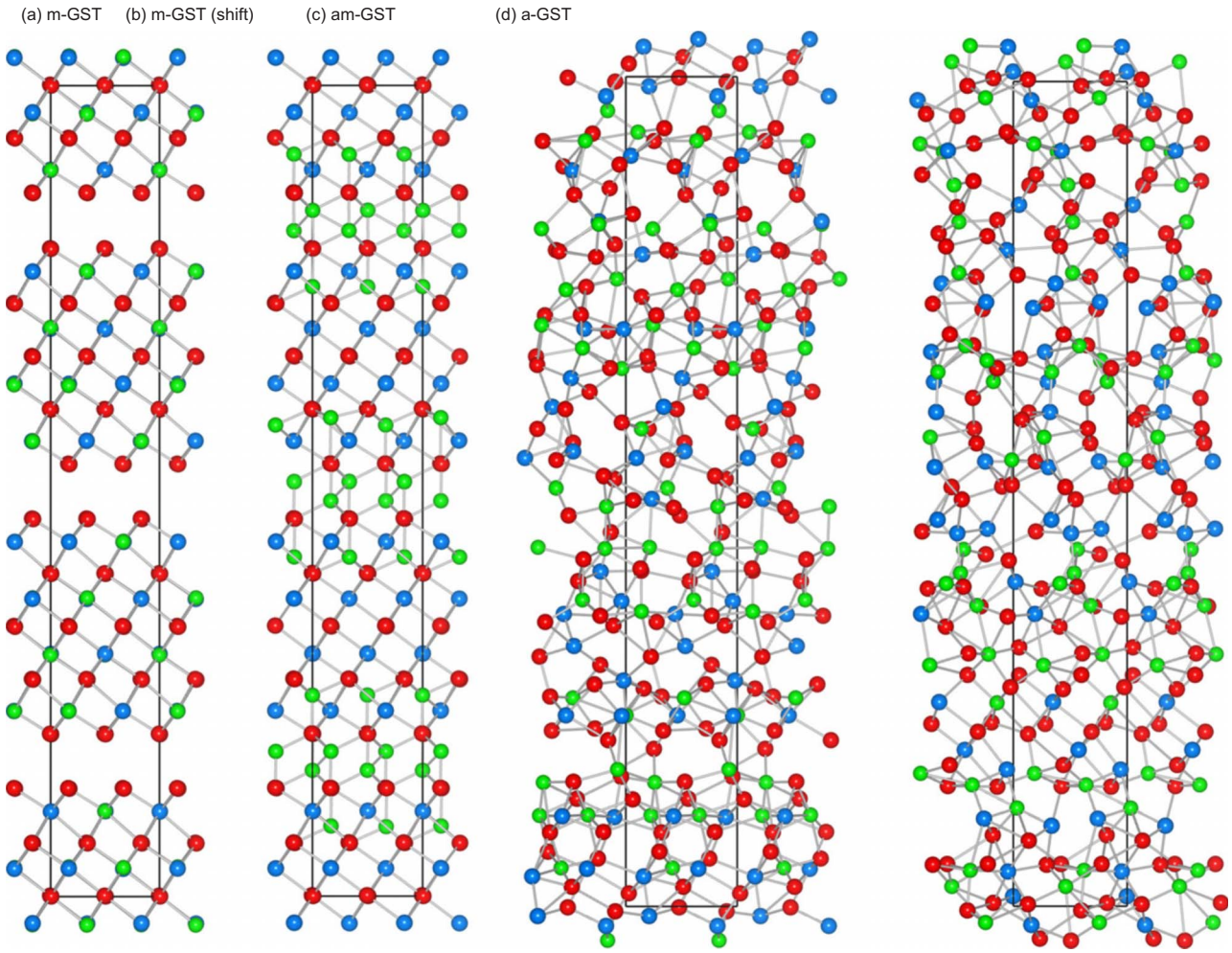

FIG. 1. (Color online) Structure models of the GST phases. (a) Metastable crystalline GST (m-GST). (b) Intermediate m-GST (shift) structure, in which the Ge atoms occupy the fourfold tetrahedron sites with lowest energy. (c) Amorphous GST obtained at zero temperature using modified m-GST structures (am-GST), in which the tetrahedron sites were initially occupied. (d) Amorphous GST obtained by high temperature MD DFT calculations (a-GST). The Ge, Sb, and Te atoms are indicated in green (light gray), blue (medium gray), and red (dark gray), respectively.

3.2 ± 0.3 Å ($\Delta_b = 0.29$ Å) for Sb–Te. We want to point out that structure models for m-GST using the same hexagonal $(2 \times 2 \times 5)$ cell, however, with only one atomic species per (111) plane, yield a unique bond length for Ge–Te and Sb–Te, which was also reported by previous calculations[40,42] and inconsistent with experimental results. It is interesting to note that two bond lengths are also present in bulk GeTe,[32,51,52] as well as in Sb_2Te_3.[32] Compared with the experimental results reported by Kolobov *et al.*,[37] the deviations (overestimation) of the calculated results are about 1.4–3.1%, in which the largest error (3.1%) is for the longest bond length of Sb–Te. However, we should note that the experimental error bar is 0.3 Å for this particular bond length, i.e., an uncertainty of about 10% in the longest Sb–Te distance. Therefore, within the errors present in DFT-PBE and the experimental studies, the agreement is excellent.

The formation of a sequence of short and long bong lengths as mentioned above can be explained by a Peierls-type electronic instability and through the presence of intrinsic vacancies.[74,75] Thus, our results support a RS-type structure for m-GST in which the Ge, Sb, and Te atoms are slightly shifted from their high-symmetry positions in a correlated manner, confirming the Kolobov *et al.*[37] suggestion.

B. Intermediate phase between crystalline and amorphous

As mentioned in the Introduction, the phase transition from m-GST to a-GST goes through a liquidlike high energy state,[3,5,10–14] which is usually achieved by a high intense and focused laser beam. Thus, the key point to obtain an atom-level understanding of the phase transition mechanism is to identify a high energy intermediate configuration that exists in between both phases.

In the lowest energy m-GST structure discussed above, the Ge and Sb atoms are sixfold coordinated; however, it has been reported that up to one-fifth of the Ge atoms are fourfold coordinate with Te atoms ($GeTe_4$) in the a-GST phase, while the remaining Ge atoms form fourfold structures with combined Ge, Sb, and Te atoms.[59] An analysis of the RS m-GST structure shows that tetrahedral Ge atoms surrounded by Te atoms can be obtained by shifting Ge along the RS [111] or $[\bar{1}\bar{1}\bar{1}]$ directions (hexagonal c axis), Fig. 1(a). It is well known that GeTe in the zincblende (ZB) structure has a higher energy than the RS structure; hence, the occupation of the tetrahedron sites in m-GST by Ge atoms can lead to high energy intermediate configurations. We want to point out that

a large number of tetrahedral sites with different local environments are present in the lowest energy RS m-GST structure, which leads to a large number of possible high energy configurations.

Thus, in order to identify the distribution of the Ge atoms in the lowest energy state among the high energy configurations, we calculated the energetics for the occupation of the tetrahedral sites with different local environments by Ge atoms. We found that the lowest energy tetrahedron sites are located in the intrinsic vacancy regions, while the highest energy sites are located in the center of the GST building blocks; i.e., there is a strong preference for the fourfold Ge atoms to be located in or near intrinsic vacancy regions. These findings provide a possible path for the displacement of the Ge atoms: Assuming that all the Ge atoms are shifted from their octahedron sites and occupy the lowest energy tetrahedron sites, we find that 50% of Ge will shift from the octahedra to tetrahedra sites along the [111] direction, while the remaining 50% Ge atoms shift along the opposite direction. This leads to a high energy configuration, which is higher in energy than the m-GST and a-GST phases. The m-GST (shift) structure in which all Ge atoms occupy the tetrahedral sites according to the distribution of the intrinsic vacancies is shown in Fig. 1(b). We want to point out that this high energy configuration is not unique as it depends also on the distribution of the intrinsic vacancies.

It can be seen that this high energy configuration leads to the formation of Ge–Ge bonds, which has been reported by experimental studies of the amorphous phase.[59] Furthermore, this configuration is unstable; i.e., the system will relax without an energy barrier to a lower energy configuration (see below). Therefore, this key finding can be used to identify the possibility of generating disordered structures by a standard geometric optimization of high energy configurations with occupation of the tetrahedral sites by Ge atoms. In principle, this high energy configuration can be achieved by an intense laser pulse, which provides enough energy for the Ge atoms to overcome the natural energy barriers that separate the octahedron and tetrahedron sites in m-GST.

C. Amorphous GST phase

In this section, we will show that a transition between the m-GST and a-GST phases can be obtained by using the high energy intermediate configurations as a link between both phases. In order to prove our concept, we first generate a-GST structures using standard first-principles MD simulations at high temperatures (high-T) to remove any structure history and a set of consecutive steps to lower the temperature. This approach is identical to the approach adopted in previous a-GST studies, and has been proved very successful in the study of the a-GST phase.[42,50,56,57]

Alternatively, we generated a-GST models from high energy structures obtained by modifying the lowest energy m-GST structure. The high energy configurations are obtained by occupying a percentage of the tetrahedron sites by Ge atoms instead of the octahedron sites. The goal is to show that a-GST structures obtained by performing a simple relaxation of the high energy configurations can preserve most of the structural features present in the a-GST generated by MD simulations, and therefore provide solid evidence to support and identify the structure mechanisms that determines the phase transition. There are a large number of possible high energy configurations and it is unclear which of them can lead to the best amorphous phase relative to experiment. As such, we performed calculations for a very large number of high energy structures, i.e., with different percentages of occupation of the tetrahedron sites by Ge atoms as well as by using different distributions.

For all high energy m-GST configurations, as well as for the selected snapshots selected along the MD simulations, we performed a complete geometric optimization of the volume and internal forces using stress tensor. Using this procedure, we will be able to take the volume changes in amorphization as a fingerprint in which to compare our multiple configurations and potential pathways against experimental results.[10,36,62]

First, we compared the a-GST structures generated using cubic and hexagonal unit cells from high temperature MD simulations. The pair correlation functions for all pairs of atoms (Ge–Te, Ge–Sb, Sb–Te, Ge–Ge, Sb–Sb, and Te–Te) were obtained by averaging the pair correlation functions over about ten structures for both unit cells. The results are shown in Fig. 2(a). We found that the agreement between both unit cells is excellent, and hence, the use of the hexagonal cell does not compromise the quality of the results even that the unit cell has a finite size. Furthermore, we compare our pair correlation functions with other first-principles MD simulations performed by Akola *et al.*[42,46,76] using larger unit cells. Our simulations reproduce all the important geometric features present in their simulations; however, minor differences can be observed, which can be attributed to the cell size. However, those minor differences do not compromise our conclusions reported in this work. The reported pair correlation functions are also consistent with experimental results (see Table I). We want to emphasize that simulations using both cells reproduce the well established volume expansion of the amorphous phase reported by experimental results. We can conclude that MD simulations yield a-GST structures with high quality and can be used as a reference to identify the structure link between the m-GST and a-GST phases.

The a-GST structures obtained by MD simulations and by geometric relaxation of the high energy m-GST phase are shown in Figs. 1(d) and 1(c), respectively. We see that, indeed, similar structural features occur in each case. Furthermore, even minor features are well described by both structures, with the formation of Ge–Ge bonds and cavity regions, both of which have been identified as key characteristics of a-GST.[42,50,55,56] In order to perform a quantitative comparison, the pair correlation functions are shown in Fig. 2(b). For the a-GST structures, the pair correlation functions were averaged over ten structures, while the pair correlation functions of the am-GST structures were calculated for ten structures with different initial occupations of the Ge tetrahedron sites; the structure that provided the best agreement with the a-GST pair correlation functions is shown in Fig. 2.

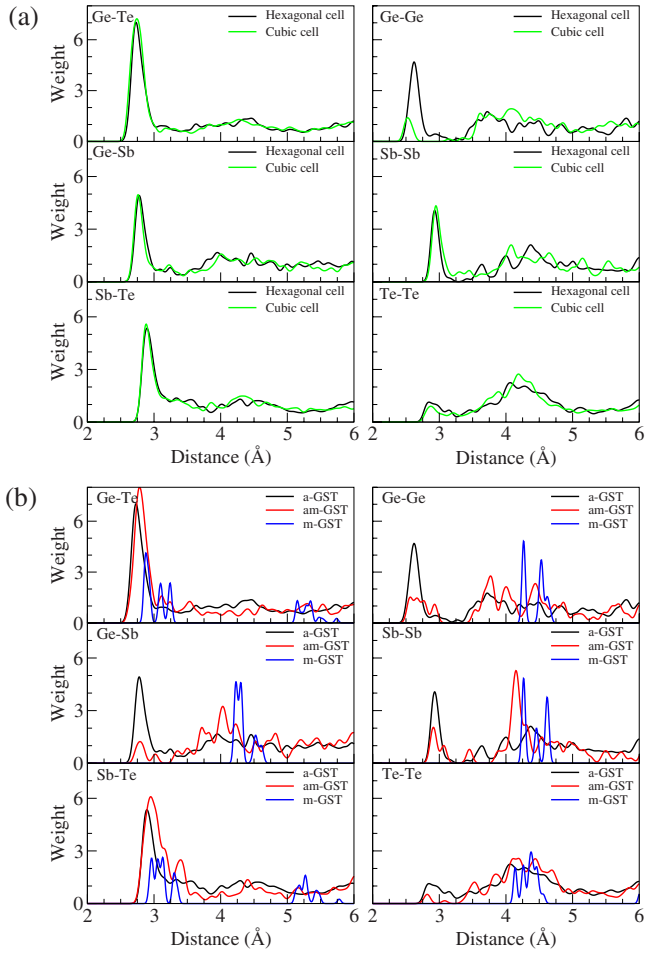

FIG. 2. (Color online) Pair correlation functions of various GST phases. (a) Amorphous GST obtained by MD calculations (a-GST) using hexagonal (black lines) and cubic (green) supercells. (b) Amorphous GST obtained by MD calculations (a-GST, black lines). Amorphous GST obtained from occupation of tetrahedron sites in m-GST and complete relaxation (am-GST, red lines). Metastable GST phase (m-GST, blue lines, scaled by 0.50).

Our PC function analysis shows that for all the am-GST structures, the one in which 50% of the Ge atoms are shifted from the octahedron to the tetrahedron sites along the hexagonal [111] direction and the remaining 50% move along the $[\bar{1}\bar{1}\bar{1}]$ direction reproduces almost all features present in the PC functions of a-GST, although some minor differences still exist. For example, for Ge–Sb and Ge–Ge PC functions, MD simulated a-GST yields more Ge–Sb and Ge–Ge pairs at about 2.79 and 2.63 Å, than in the am-GST structure. Thus, the present analysis suggest that the occupation of the tetrahedron sites by Ge atoms leads to a high energy configuration that serves as the intermediate link between the crystalline and amorphous phases.

We observed that only the am-GST structures in which the Ge atoms initially occupy fourfold sites in or near the intrinsic vacancies lead to structure properties in good agreement with the calculated MD a-GST structures. Thus, it suggests that the location of the intrinsic vacancies plays an important role in the phase transition, which can be explained by the lower energy barriers for Ge displacements close to intrinsic vacancy regions. Furthermore, we observe that am-GST structures in which less than half of the Ge atoms are moved to the tetrahedron sites do not yield PC functions similar to the a-GST structures, instead they show strong similarity to the PC function calculated for m-GST (see Fig. 2). For the lowest energy m-GST structures, in which the intrinsic vacancies are ordered in a plane perpendicular to *c*, our results indicate that all the Ge atoms will shift. However, at high temperature or under nonequilibrium growth conditions the intrinsic vacancies may distribute more randomly among the cation sites, which is expected to play an important role in the pattern of shifting Ge atoms from their stable octahedra.

TABLE I. Bond lengths (in angstroms) of GST in the amorphous and crystalline phases.

	Amorphous GST			Metastable GST	
	a-GST	am-GST	Expt.	m-GST	Expt.
Ge–Te	2.74	2.79	2.60–2.63[a]	2.87–3.24	2.83–3.15[b]
Sb–Te	2.91	2.96	2.82–2.85[a]	2.96–3.30	2.91[b]
Te–Te	4.16	4.28		4.14–4.38	4.26[b]
Ge–Ge	2.63	2.64	2.47–2.48[a]	4.27–4.62	
Ge–Sb	2.79	2.78	2.69[a]	4.23–4.53	
Sb–Sb	2.93	2.92		4.27–4.62	

[a]Experimental: Refs. 55 and 59.
[b]Experimental: Refs. 37 and 54.

1. Volume expansion of the amorphous GST phase

As previously mentioned, the volume expansion of the a-GST phase upon the transition can be used as a fingerprint to assess the quality of our a-GST structures. Using the calculated equilibrium volumes by stress tensor, we obtained a density of 5.89 g/cm^3 for m-GST, while for the MD a-GST structures, we found 5.41 and 5.35 g/cm^3 employing the cubic and hexagonal cells, i.e., a difference of about 1% due to the cell shape. The results for the MD a-GST structures were obtained by averaging over ten volumes in both cases. For the am-GST structures, we obtained 5.36 g/cm^3 for the am-GST that yields the best PC function in agreement with the MD a-GST PC functions. The agreement is excellent between both amorphous densities, which provide further support for the identification of a structure link between both crystalline and amorphous phases.

Therefore, we found a decrease in the amorphous density upon amorphization compared with the crystalline m-GST phase of 8.1%–9.2%. Thus, it implies a volume expansion of about 9.0%–10%, which is larger than the volume expansion reported by experimental studies (6.4%).[36] The volume expansion upon amorphization is a consequence of the Ge atoms moving from high coordination environments to the lower coordination sites in the a-GST structures. A similar trend occurs in amorphous GeTe. Therefore, the smaller volume deformation observed in the experimental sample may indicate that the amorphization process in not complete;[3,59] i.e., not all the Ge atoms are moved away from their stable octahedron sites. Thus, within those deviations, our model structures obtained using different approaches are consistent with experimental results.

2. Relative total energy differences between crystalline and amorphous phases

Relative energy difference of 28–42 meV/at. between the crystalline and amorphous phases has been extrapolated from differential scanning calorimetry measurements.[63] This can be employed as a second reference to assess the quality of our results. Total energy calculations reveal that the MD a-GST structures are about 140–182 meV/at. higher in energy than the lowest energy m-GST structure, which corresponds to the upper energy limit between the fully amorphized a-GST and the ordered m-GST structure. In the lowest energy m-GST, the intrinsic vacancies are ordered in (111) planes perpendicular to the [111] direction.

It is important to notice, as mentioned above, that the m-GST structure might not be fully ordered and the a-GST might not be fully amorphized. To test these suggestions, we calculated the total energy of m-GST with a disordered distribution of the intrinsic vacancies, while we keep an ordered distribution for the Ge, Sb, and Te atoms. Using this structure as a reference configuration, we found a relative energy difference between the a-GST and m-GST of about 110–151 meV/at., i.e., a decrease of about 30 meV/at. The energy difference could be further reduced to about 50 meV/at. if only a fraction of the Ge atoms undergo site transitions. Thus, again, this analysis suggests that a full scale amorphorization of GST or complete ordering of Ge, Sb, and intrinsic vacancies in m-GST may not be typical in the experimental GST samples, and our calculations represent the fully disordered and ordered limits, respectively.

3. Bond lengths in the amorphous GST phase

The averaged bond lengths calculated for both phases are summarized in Table I along with available experimental results.[37,54,55,59] The calculated bond lengths deviate by about 3%–6% from the experimental results; a feature mostly due to the use of GGA in our calculations, which systematically overestimates the lattice constants by about 3%.[72,77,78] Furthermore, it is important to notice that the nearest-neighbor distances are spread over a large range of values; e.g., Ge–Te is from 2.67 to 2.94 Å and Sb–Te is from 2.86 to 3.23 Å. We found a contraction in the averaged Ge–Te bond lengths in a-GST of up to 10% compared with m-GST; e.g., Ge–Te decreases from 2.87–3.24 (m-GST) to 2.67–2.94 Å (a-GST), while experimental measurements obtained a decrease of about 12%. Similar trends exist for Sb–Te.

4. Instability of the ZB GeTe phase

To understand the disorder effects introduced by the shift of Ge atoms from octahedron to tetrahedron sites, we calculated the potential energy path along the RS [111] direction for GeTe as a function of Ge shift from octahedron (perfect RS) to the tetrahedron (ZB) sites. The results are shown in Fig. 3. As expected, the distorted RS structure has the lowest energy (54 meV lower than the perfect RS structure), in which the distortion is driven by Peierls-type level repulsion near the band edge. Unexpectedly, the ZB structure in which the Ge atoms occupy the tetrahedron sites with bond angles (Ge–Te–Ge) of 109.47° is not a local minimum as would be

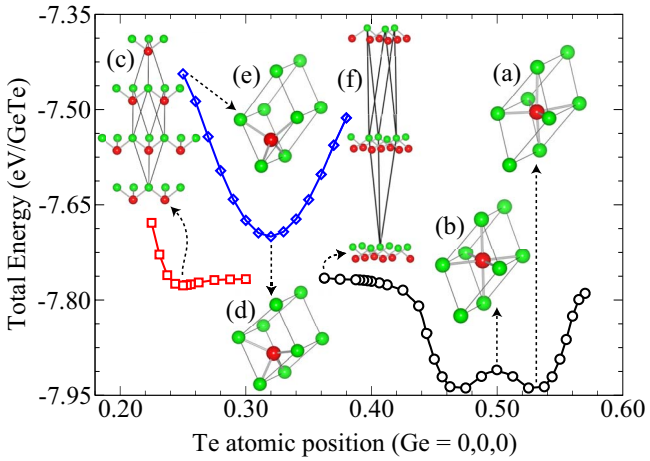

FIG. 3. (Color online) Potential energy path for atomic displacements of Ge atoms along of the RS [111] direction of GeTe. (a) Distorted RS structure. (b) Perfect RS structure. (c) Long Ge–Te bond ZB structure. (d) Graphitelike structure. (e) Perfect ZB structure. (f) RS-layer structure.

expected based on the general trends for binary semiconductors. In fact, we found that the ZB structure relaxes without an energy barrier to the "graphitelike" or to the "long-Ge–Te" structures, which have lower energies than the high-symmetry ZB phase. Thus, Ge at ideal tetrahedral sites are intrinsically unstable in GeTe, which drives the Ge atoms at tetrahedral sites in GST to move away and adopt a variety of lower symmetry coordination environments.

The variety of coordination environments found in the GeTe energy surface is remarkable. For Ge site coordination of (0.25,0.25,0.25)–(0.40,0.40,0.40), three structures have similar energies, i.e., long-Ge–Te, layered-ZB, and layered-RS. In long-Ge–Te, the Ge atoms form three short bonds (2.77 Å) and one *long* bond (4.68 Å) with the Te atoms. However, Ge is only threefold coordinated in the layered structures with bond lengths of 2.76 Å, which is 2.90% (14.51%) smaller than the short (longer) Ge–Te bond lengths in the distorted RS structure. As the layered GeTe structures are lower in energy than the graphitelike phase and only about 100 meV/f.u. higher than the distorted RS structure, it indicates a strong tendency of Ge atoms to form fourfold motifs with three short-Ge–Te bonds (about 2.76 Å) and bond angles of about 90°. Similar results, e.g., short bond lengths and average bond angles of about 90°, are observed by our calculations for a-GST, which is also consistent with previous MD results for a-GST,[42,50,56] as well as by experimental observations.[37,54,59,79] Therefore, the inherent instability of Ge at the tetrahedral sites, low displacement energy, and unique coordination preferences of GeTe plays an important role in the formation of a-GST.

Using the structural links between the m-GST and a-GST phases identified above, it is possible now to explain why there is no direct phase transition from s-GST to a-GST phases. The Te atoms have a different stacking sequence in the s-GST and m-GST structures. The altered stacking sequence in s-GST breaks the RS symmetry and limits the shift of the Ge atoms along the hexagonal [0001] direction to the tetrahedron sites in the intrinsic vacancy regions. This

stresses the role played by the intrinsic vacancies as well as by the instability of the tetrahedron sites in the m-GST structures.

Our results and analysis lead to the conclusion that the rapid phase change in GST originates from the synergistic combination of properties from GeTe and Sb_2Te_3. Sb_2Te_3 provides intrinsic lattice vacancies and its energy in the RS structure is only 3 meV/at. higher than the stable rhombohedral structure, thus contributes to the formation of the metastable RS-type structures. GeTe contributes its RS-type structure in which Ge displacements along the RS [111] direction can be realized at low energy cost. The instability at the tetrahedral sites leads to the generation of disordered GST structures in which the Ge atoms are mostly fourfold coordinated with three short-Ge–Te bond lengths. As the displacement has the lowest energy near intrinsic vacancy sites, our analysis suggests that a high degree of amorphization can be achieved most easily when the system has a composition of $(GeTe)_2(Sb_2Te_3)$, in which the number of Ge atoms and Te tetrahedron sites matches that of the vacancy sites. This is consistent with the observation that GST has the highest figure of merit of all Ge–Sb–Te compounds.

IV. SUMMARY

In summary, using first-principles calculations, we obtained a direct structural link between the metastable and amorphous GST phases. We found that a shift of the Ge atoms along the RS [111] direction (hexagonal [0001] direction) leads to a high energy intermediate configuration between the m-GST and a-GST phases. The intermediate phase is characterized by a large amount of tetrahedra sites occupied by Ge atoms, which are unstable as in the parent GeTe structure. The natural relaxation of the intermediate configuration leads to the generation of disordered GST structures in which the Ge atoms are mostly fourfold coordinated with three short-Ge–Te bond lengths. The tetrahedra sites near the intrinsic vacancies sites are occupied first by Ge atoms due to the lower energy barriers; hence, the high energy intermediate configuration is not unique and depends on the initial conditions provided by the m-GST phase.

We find that the high figures of merit can be achieved most easily when the system has a composition of $(GeTe)_2(Sb_2Te_3)$ due to the ideal match of the number of intrinsic vacancies provided by Sb_2Te_3 and instability of the Ge tetrahedron sites provided by GeTe in its RS-type structure. This is because the displacement has the lowest energy near intrinsic vacancy sites, thus a high degree of amorphization when the number of intrinsic vacancies and the Ge tetrahedron sites match. These results provide an alternative understanding of the phase change process in GST and will be important to guide experimental efforts for the improved performance and design of future phase change materials.

ACKNOWLEDGMENTS

The work at the NREL was supported by the U.S. Department of Energy (DOE) under Contract No. DE-AC36-08GO28308. Computing resources of the National Energy Research Scientific Computing Center were employed, which is supported by the DOE under Contract No. DE-AC02-05CH11231. J.L.F.D. thanks also the São Paulo Science Foundation (FAPESP).

[1] G. I. Meijer, Science **319**, 1625 (2008).
[2] S. R. Ovshinsky, Phys. Rev. Lett. **21**, 1450 (1968).
[3] N. Yamada, E. Ohno, K. Nishiuchi, N. Akahira, and T. Takao, J. Appl. Phys. **69**, 2849 (1991).
[4] I. Friedrich, V. Weidenhof, W. Njoroge, P. Franz, and M. Wuttig, J. Appl. Phys. **87**, 4130 (2000).
[5] M. Wuttig and N. Yamada, Nature Mater. **6**, 824 (2007).
[6] T. C. Chong, L. P. Shi, X. Q. Wei, R. Zhao, H. K. Lee, P. Yang, and A. Y. Du, Phys. Rev. Lett. **100**, 136101 (2008).
[7] D. Wamwangi, W. K. Njoroge, and M. Wuttig, Thin Solid Films **408**, 310 (2002).
[8] D.-S. Suh, E. Lee, K. H. P. Kim, J.-S. Noh, W.-C. Shin, Y.-S. Kang, C. Kim, Y. Khang, H. R. Yoon, and W. Jo, Appl. Phys. Lett. **90**, 023101 (2007).
[9] W.-D. Song, L.-P. Shi, X.-S. Miao, and C.-T. Chong, Adv. Mater. **20**, 2394 (2008).
[10] V. Weidenhof, I. Friedrich, S. Ziegler, and M. Wuttig, J. Appl. Phys. **86**, 5879 (1999).
[11] B. J. Kooi, W. M. G. Groot, and J. T. M. De Hosson, J. Appl. Phys. **95**, 924 (2004).
[12] T. Matsunaga and N. Yamada, Jpn. J. Appl. Phys., Part 1 **43**, 4704 (2004).
[13] W. J. Wang, R. Zhao, L. P. Shi, X. S. Miao, P. K. Tan, M. H. Hong, T. C. Chong, Y. H. Wu, and Y. Lin, J. Appl. Phys. **98**, 124313 (2005).
[14] W. Braun, R. Shayduk, T. Flissikowski, M. Ramsteiner, H. T. Grahn, H. Riechert, P. Fons, and A. Kolobov, Appl. Phys. Lett. **94**, 041902 (2009).
[15] X. S. Miao, T. C. Chong, Y. M. Huang, K. G. Lim, P. K. Tan, and L. P. Shi, Jpn. J. Appl. Phys., Part 1 **38**, 1638 (1999).
[16] T. Kato and K. Tanaka, Jpn. J. Appl. Phys., Part 1 **44**, 7340 (2005).
[17] B.-S. Lee, J. R. Abelson, S. G. Bishop, D.-H. Kang, B.-K. Cheong, and K.-B. Kim, J. Appl. Phys. **97**, 093509 (2005).
[18] J. K. Olson, H. Li, T. Ju, J. M. Viner, and P. C. Taylor, J. Appl. Phys. **99**, 103508 (2006).
[19] W. Welnic, S. Botti, L. Reining, and M. Wuttig, Phys. Rev. Lett. **98**, 236403 (2007).
[20] J.-W. Park, S. H. Back, T. D. Kang, H. Lee, Y.-S. Kang, T.-Y. Lee, D.-S. Suh, K. J. Kim, C. K. Kim, Y. H. Khang *et al.*, Appl. Phys. Lett. **93**, 021914 (2008).
[21] K. Shportko, S. Kremers, M. Woda, D. Lencer, J. Robertson, and M. Wuttig, Nature Mater. **7**, 653 (2008).
[22] J.-W. Park, S. H. Eom, H. Lee, J. L. F. Da Silva, Y.-S. Kang, T.-Y. Lee, and Y. H. Khang, Phys. Rev. B **80**, 115209 (2009).
[23] K. A. Agaev and A. G. Talybov, Sov. Phys. Crystallogr. **11**, 400 (1966).
[24] I. I. Petrov, R. M. Imamov, and Z. G. Pinsker, Sov. Phys. Crystallogr. **13**, 339 (1968).
[25] O. G. Karpinsky, L. E. Shelimova, M. A. Kretova, and J.-P. Fleurial, J. Alloys Compd. **268**, 112 (1998).
[26] L. E. Shelimova, O. G. Karpinskii, M. A. Kretova, V. I. Kosyakov, V. A. Shestakov, V. S. Zemskov, and F. A. Kuznetsov, Inorg. Mater. **36**, 768 (2000).
[27] B. J. Kooi and T. T. M. De Hosson, J. Appl. Phys. **92**, 3584 (2002).
[28] T. Matsunaga and N. Yamada, Phys. Rev. B **69**, 104111 (2004).
[29] T. Matsunaga, N. Yamada, and Y. Kubota, Acta Crystallogr. B **60**, 685 (2004).
[30] T. Matsunaga, R. Kojima, N. Yamada, K. Kifune, Y. Kubota, and M. Takata, Appl. Phys. Lett. **90**, 161919 (2007).
[31] T. Matsunaga, H. Morita, R. Kojima, N. Yamada, K. Kifune, Y. Kubota, Y. Tabata, J.-J. Kim, M. Kobata, E. Ikenaga *et al.*, J. Appl. Phys. **103**, 093511 (2008).
[32] J. L. F. Da Silva, A. Walsh, and H. Lee, Phys. Rev. B **78**, 224111 (2008).
[33] T. Nonaka, G. Ohbayashi, Y. Toriumi, Y. Mori, and H. Hashimoto, Thin Solid Films **370**, 258 (2000).
[34] N. Yamada and T. Matsunaga, J. Appl. Phys. **88**, 7020 (2000).
[35] T. Matsunaga and N. Yamada, Jpn. J. Appl. Phys., Part 1 **41**, 1674 (2002).
[36] W. K. Njoroge, H.-W. Wöltgens, and M. Wuttig, J. Vac. Sci. Technol. A **20**, 230 (2002).
[37] A. V. Kolobov, P. Fons, J. Tominaga, A. I. Frenkel, A. L. Ankudinov, S. N. Yannopoulos, K. S. Andrikopoulos, and T. Uruga, Jpn. J. Appl. Phys., Part 1 **44**, 3345 (2005).
[38] Y. J. Park, J. Y. Lee, M. S. Youm, Y. T. Kim, and H. S. Lee, J. Appl. Phys.

97, 093506 (2005).
[39]J.-H. Eom, Y.-G. Yoon, C. Park, H. Lee, J. Im, D.-S. Suh, J.-S. Noh, Y. Khang, and J. Ihm, Phys. Rev. B **73**, 214202 (2006).
[40]Z. Sun, J. Zhou, and R. Ahuja, Phys. Rev. Lett. **96**, 055507 (2006).
[41]W. Welnic, A. Pamungkas, R. Detemple, C. Steimer, S. Blügel, and M. Wuttig, Nature Mater. **5**, 56 (2006).
[42]J. Akola and R. O. Jones, Phys. Rev. B **76**, 235201 (2007).
[43]Z. Sun, S. Kyrsta, D. Music, R. Ahuja, and J. M. Schneider, Solid State Commun. **143**, 240 (2007).
[44]M. Wuttig, D. Lüsebrink, D. Wamwangi, W. Welnic, M. Gillessen, and R. Dronskowski, Nature Mater. **6**, 122 (2007).
[45]J. Yu, Z. Song, B. Liu, S. Feng, and B. Chen, Jpn. J. Appl. Phys., Part 1 **46**, 4215 (2007).
[46]J. Akola and R. O. Jones, J. Phys.: Condens. Matter **20**, 465103 (2008).
[47]J. Im, J.-H. Eom, C. Park, K. Park, D.-S. Suh, K. Kim, Y.-S. Kang, C. Kim, T.-Y. Lee, Y. Khang *et al.*, Phys. Rev. B **78**, 205205 (2008).
[48]M.-C. Jung, K.-H. Kim, Y.-M. Lee, J.-H. Eom, J. Im, Y.-G. Yoon, J. Ihm, S. A. Song, H.-S. Jeong, and H.-J. Shin, J. Appl. Phys. **104**, 074911 (2008).
[49]G. Lee and S.-H. Jhi, Phys. Rev. B **77**, 153201 (2008).
[50]J. Hegedüs and S. R. Elliott, Nature Mater. **7**, 399 (2008).
[51]T. Chattopadhyay, J. X. Boucherle, and H. G. von Schnering, J. Phys. C **20**, 1431 (1987).
[52]A. V. Kolobov, J. Tominaga, P. Fons, and T. Uruga, Appl. Phys. Lett. **82**, 382 (2003).
[53]M. Först, T. Dekorsy, C. Trappe, M. Laurenzis, H. Kurz, and B. Béchevet, Appl. Phys. Lett. **77**, 1964 (2000).
[54]A. V. Kolobov, P. Fons, A. I. Frenkel, A. L. Ankudinov, J. Tominaga, and T. Uruga, Nature Mater. **3**, 703 (2004).
[55]D. A. Baker, M. A. Paesler, G. Lucovsky, S. C. Agarwal, and P. C. Taylor, Phys. Rev. Lett. **96**, 255501 (2006).
[56]S. Caravati, M. Bernasconi, T. D. Kühne, M. Krack, and M. Parrinello, Appl. Phys. Lett. **91**, 171906 (2007).
[57]Z. Sun, J. Zhou, and R. Ahuja, Phys. Rev. Lett. **98**, 055505 (2007).
[58]D. Ielmini, S. Lavizzari, D. Sharma, and A. L. Lacaita, Appl. Phys. Lett. **92**, 193511 (2008).
[59]P. Jóvári, I. Kaban, J. Steiner, B. Beuneu, A. Schöps, and M. A. Webb, Phys. Rev. B **77**, 035202 (2008).
[60]Z. Sun, J. Zhou, A. Blomqvist, B. Johansson, and R. Ahuja, Phys. Rev. Lett. **102**, 075504 (2009).
[61]K. S. Andrikopoulos, S. N. Yannopoulos, G. A. Voyiatzis, A. V. Kolobov, M. Ribes, and J. Tominaga, J. Phys.: Condens. Matter **18**, 965 (2006).
[62]T. P. L. Pedersen, J. Kalb, W. Njoroge, D. Wamwangi, and M. Wuttig, Appl. Phys. Lett. **79**, 3597 (2001).
[63]J. Kalb, F. Spaepen, and M. Wuttig, J. Appl. Phys. **93**, 2389 (2003).
[64]D. Lee, S. S. Lee, W. Kim, C. Hwang, M. B. Hossain, N. L. Hung, H. Kim, C. G. Kim, H. Lee, H. N. Hwang *et al.*, Appl. Phys. Lett. **91**, 251901 (2007).
[65]P. Hohenberg and W. Kohn, Phys. Rev. **136**, B864 (1964).
[66]W. Kohn and L. J. Sham, Phys. Rev. **140**, A1133 (1965).
[67]J. P. Perdew, K. Burke, and M. Ernzerhof, Phys. Rev. Lett. **77**, 3865 (1996).
[68]P. E. Blöchl, Phys. Rev. B **50**, 17953 (1994).
[69]G. Kresse and D. Joubert, Phys. Rev. B **59**, 1758 (1999).
[70]G. Kresse and J. Hafner, Phys. Rev. B **48**, 13115 (1993).
[71]G. Kresse and J. Furthmüller, Phys. Rev. B **54**, 11169 (1996).
[72]M. Fuchs, J. L. F. Da Silva, C. Stampfl, J. Neugebauer, and M. Scheffler, Phys. Rev. B **65**, 245212 (2002).
[73]J. L. F. Da Silva, C. Stampfl, and M. Scheffler, Surf. Sci. **600**, 703 (2006).
[74]J. K. Burdett and S. Lee, J. Am. Chem. Soc. **105**, 1079 (1983).
[75]J.-P. Gaspard, F. Marinelli, and A. Pellegatti, Europhys. Lett. **3**, 1095 (1987).
[76]J. Akola and R. O. Jones, Phys. Rev. Lett. **100**, 205502 (2008).
[77]J. L. F. Da Silva, S.-H. Wei, J. Zhou, and X. Wu, Appl. Phys. Lett. **91**, 091902 (2007).
[78]J. L. F. Da Silva, M. V. Ganduglia-Pirovano, J. Sauer, V. Bayer, and G. Kresse, Phys. Rev. B **75**, 045121 (2007).
[79]A. V. Kolobov, J. Haines, A. Pradel, M. Ribes, P. Fons, J. Tominaga, Y. Katayama, T. Hammouda, and T. Uruga, Phys. Rev. Lett. **97**, 035701 (2006).